Statistical Prediction of Spectrum Occupancy Perception in Dynamic Spectrum Access Networks

Miguel López-Benítez and Fernando Casadevall
Department of Signal Theory and Communications
Universitat Politècnica de Catalunya (UPC)
Barcelona, Spain
Email: {miguel.lopez, ferranc}@tsc.upc.edu

***Abstract*—Cognitive radio nodes of a dynamic spectrum access network monitor the spectrum around them in order to detect and opportunistically exploit temporarily unoccupied spectrum gaps. The overall behavior of the whole network depends on the spectrum occupancy perceived by each node at its local environment. An appropriate understanding of the local perception of cognitive radio nodes in various scenarios and locations as well as its dependence on the propagation environment can provide valuable information for the design, dimensioning and performance evaluation of dynamic spectrum access networks. In this context, this work presents a novel and practical approach to predict the spectrum occupancy that would be perceived by cognitive radio nodes in realistic scenarios. Based on such approach, we explore the dependence of the spectrum occupancy perception with the considered scenario and location as well as the impact of particular parameters of the radio environment.**

I. Introduction

The increasing spectrum demand growth experienced during the last years has lead to a virtual spectrum scarcity problem. This situation, however, actually results from the inflexible and inefficient spectrum access policies currently employed in most regulatory regimes rather than the depletion of spectrum, as it has been demonstrated by many spectrum measurement campaigns [1–6]. This circumstance has motivated the emergence of Dynamic Spectrum Access (DSA) policies based on the Cognitive Radio (CR) technology [7]. The basic underlying principle of DSA/CR is to allow unlicensed users to access in an opportunistic and non-interfering manner some licensed bands temporarily unoccupied by licensed users. Unlicensed (secondary) CR terminals monitor the spectrum in order to detect spectrum gaps left unused by licensed (primary) users and opportunistically transmit. Secondary unlicensed transmissions are allowed according to this operating principle as long as they do not result in harmful interference to the licensees.

The behavior of a DSA/CR network, and consequently its impact on the primary network performance, strongly depends on the spectrum occupancy perceived by each CR node at its local environment. The possibility of estimating the user's perceived spectrum occupancy at different realistic locations as a function of the considered scenario and the surrounding radio propagation environment can provide a valuable tool for the design, dimensioning and performance evaluation of DSA/CR networks. A realistic and accurate estimation of such perception becomes therefore essential and extremely useful in the domain of DSA/CR research.

The impact of considering various scenarios and propagation environments on the perceived spectrum occupancy could be estimated by means of field measurements performed at different locations. Based on experimental measurements, it is possible to infer how different operating conditions affect the perceived spectrum occupancy. As an example, the study carried out in [8] performed a multi-band spectrum measurement campaign and evaluated the percentage of time that various bands were observed as busy over a wide diversity of practical scenarios including indoor locations, outdoor high points and outdoor locations at the ground level (in open areas and between buildings). The main advantage of field measurement-based approaches is that they implicitly account for all the potential propagation phenomena and affecting factors present in real environments. However, the user's perception as a function of the considered scenario and propagation environment can be characterized in a merely qualitative manner since the impact of particular factors or parameters (e.g., primary transmission power, operating frequency, building height, street width, etc.) cannot be isolated and quantified separately.

Another alternative approach would consist on the use of appropriate radio propagation models in order to predict the primary signal power that would be received at various locations. Assuming that CR nodes decide on spectrum use based on energy detection[1], the power levels predicted by the propagation model would be compared to a properly set decision threshold[2] in order to determine if the CR node would observe the sensed spectrum as busy at the considered location. Notice that this approach enables the impact of every factor or parameter considered by the propagation model to be analyzed and quantified separately. However, this method results in an oversimplified characterization of the perceived occupancy where spectrum at a given location is always observed either as busy or idle. In practice, radio propagation phenomena such as fast (multipath) fading or slow (shadowing) fading, provoke momentary signal fades. Under low Signal-to-Noise Ratio (SNR) conditions, which is of particular interest in the study of DSA/CR, this may sometimes result in signal misdetections, i.e. the CR node observes the spectrum as idle when it is actually being used. Thus, the probability that the spectrum is observed as busy constitutes a more appropriate parameter to characterize the spectrum occupancy perceived at various locations.

This work presents a novel and practical approach combining radio propagation models with a recently proposed model for DSA/CR in order to provide together the benefits

[1] Despite its practical performance limitations, energy detection [9] has gained popularity as a spectrum sensing technique for DSA/CR due to its general applicability and simplicity as well as its low computational and implementation costs [10, 11]. It has been a preferred approach for many past DSA/CR studies and also constitutes the sensing method considered here.

[2] In practice, the decision threshold is normally chosen to satisfy a certain probability of false alarm [12], which is defined as the probability that the channel is declared to be busy when it is actually idle. For an energy detector, a false alarm occurs when noise exceeds the decision threshold.

of the aforementioned alternatives. Firstly, the proposed approach provides a probabilistic (not binary) characterization of the spectrum occupancy that would be perceived by CR nodes for different scenarios and locations. Secondly, the impact on the perceived spectrum occupancy of particular parameters of the considered scenario and radio environment can easily be isolated, quantified and analyzed. Moreover, it is possible to include the potential propagation phenomena of real environments by means of a few input parameters that can readily be obtained experimentally in practice with common general-purpose measurement devices such as off-the-shelf spectrum analyzers, thus enabling more accurate and reliable estimations. The potentials of the proposed approach are illustrated with an application to a complex and realistic scenario in a generic urban environment.

II. Statistical Prediction Approach

The proposed statistical prediction approach (illustrated in Figure 1) makes use of radio propagation models along with a Duty Cycle (DC) model specifically devised for DSA/CR.

In the first step, the radio propagation model is used to estimate, based on a set of input parameters $\mathbf{p} = (p_1, p_2, \ldots, p_M)$ such as operating frequency, distance, etc., the radio propagation loss L between the primary transmitter and the CR receiver that is sensing the spectrum. Notice that the propagation model is neither specified nor constrained by the proposed method. Any model capable to estimate the radio propagation loss L as a function of the scenario and environment parameters $\mathbf{p}$ can be employed. This flexibility allows the selection of the propagation model that best fits the scenario under study. The parameters $\mathbf{p}$ required to estimate L are model-specific and therefore depend on the selected model.

Based on the primary transmission power P_T, the computed losses L are then employed to compute the primary power P_S that would be observed by CR nodes at various locations. The received P_S values are translated to SNR values γ by making use of the noise power P_N at the CR receiver. The resulting SNR values are then fed, along with an additional set of input parameters $\mathbf{p}' = (p'_1, p'_2, \ldots, p'_N)$, to the DC model, which outputs an estimation Ψ of the DC that would be perceived by the CR nodes at the considered geographical locations.

The DC can be defined from both empirical and probabilistic perspectives. From an empirical viewpoint, the DC can be defined as the fraction (or percentage) of time that a certain channel (or frequency range) is observed as busy by a secondary CR terminal at a given geographical location. From a probabilistic viewpoint, the DC can be defined as the probability that a certain channel (or frequency range) is observed as busy at a given geographical location. While the former definition is more appropriate for spectrum measurement campaigns and other field studies, the latter results more convenient for theoretical approaches as it is the case of this work. The interest of employing the DC lies in its ability to summarize the overall spectrum occupancy within a certain time and frequency range in a single numerical value. The DC has been employed in many past spectrum occupancy studies to quantify and compare the occupancy level of several spectrum bands, or to compare the occupancy of the same band under different conditions or at different locations. This work considers the spatial DC distribution as a mean to describe the spatial spectrum occupancy that would be perceived by CR nodes at different geographical locations.

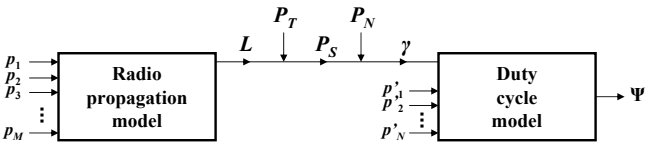

Fig. 1. Statistical prediction approach.

The perceived DC, Ψ, is computed as [13]:

$$\Psi = \left(1 - \sum_{k=1}^{K} \alpha_k\right) P_{fa} + \sum_{k=1}^{K} \alpha_k \, Q\left(\frac{Q^{-1}(P_{fa})\,\sigma_N - \gamma_k}{\sigma_{S_k}}\right) \quad (1)$$

where $K > 0$ represents the number of transmission power levels that may be present in the channel (this may be due to K constant-power primary transmitters time-sharing the channel, a single variable-power transmitter that can adequately be described with a discrete set of K transmission power levels, or a combination thereof), $0 < \alpha_k \leq 1$ is the activity factor of the k-th power level, i.e. the probability (or fraction of time) that it is present in the channel ($\sum_{k=1}^{K} \alpha_k \leq 1$), P_{fa} is the target probability of false alarm considered for the selection of the energy decision threshold, $\gamma_k(\mathrm{dB}) = P_{S_k}(\mathrm{dBm}) - P_N(\mathrm{dBm})$ is the SNR resulting from the k-th average transmission power level, σ_{S_k} and σ_N are the standard deviation in decibels of the k-th signal and noise power levels respectively, $Q(\cdot)$ is the Gaussian Q-function and $Q^{-1}(\cdot)$ is the inverse of $Q(\cdot)$. These parameters constitute the input vector $\mathbf{p}'$ in Figure 1.

As depicted in Figure 1:

$$P_{S_k}(\mathrm{dBm}) = P_{T_k}(\mathrm{dBm}) - L(\mathrm{dB}) \quad (2)$$

while P_N, which represents the CR terminal's noise floor created from the sum of all the receiver's noise sources (including thermal noise), can be expressed as:

$$P_N(\mathrm{dBm}) = -174\mathrm{dBm/Hz} + 10\log_{10} B(\mathrm{Hz}) + \mathrm{NF(dB)} \quad (3)$$

where $-174\mathrm{dBm/Hz}$ is the thermal noise power spectral density at 290K, B is the radio bandwidth of the sensed channel and NF is the CR terminal's noise figure.

The instantaneous values of signal and noise power experienced at various sensing events may suffer some fluctuations around the true mean values P_{S_k} and P_N, respectively. In the case of the instantaneous noise power, such fluctuations are due to finite sensing times, which may not be long enough to average the instantaneous oscillations of noise. In the case of the instantaneous signal power, this may additionally be due to the fading properties of the radio channel as well as the primary transmission power pattern (i.e., the primary station may be a variable-power transmitter). To account for such fluctuations, σ_{S_k} and σ_N need to be considered. Such values can be estimated or obtained experimentally in practice with common general-purpose measurement devices such as off-the-shelf spectrum analyzers. Table I shows some examples of σ_{S_k} and σ_N for various bands, which have been derived from the measurements performed in [13] in order to validate equation 1. The values correspond to channels with $K = 1$. Notice that the received signal is always affected by the receiver's noise and, as a result, $\sigma_{S_k} > \sigma_N$. From measurements, we estimated that the spectrum analyzer employed in [13] was characterized by an approximated average sweep speed of 25 ms/MHz, which results in the sensing times shown in

TABLE I
EXPERIMENTAL VALUES OF σ_{S_k} AND σ_N.

Band	B (Hz)	Sensing time (ms)	σ_{S_k} (dB)	σ_N (dB)
TV	$8 \cdot 10^6$	200	0.5252	0.1679
UMTS	$5 \cdot 10^6$	125	0.4138	0.2093
DAB-T	$1.7 \cdot 10^6$	42.5	0.8298	0.3640
GSM/DCS	$200 \cdot 10^3$	5	1.6421	0.8921
TETRA	$25 \cdot 10^3$	0.625	2.0469	1.3624

Table I. As it can be appreciated, there is a clear and direct relation between the effective sensing time per channel and the resulting σ_N. The trend is not so well-defined for σ_{S_k} because in this case the obtained values also depend on the channel fading properties at various frequencies as well as the particular transmission power pattern of each radio technology.

Before concluding this section it is worth noting, as mentioned in Section I, that the proposed approach provides a probabilistic characterization, by means of Ψ, of the spectrum occupancy that would be perceived by CR nodes for different scenarios and locations. Moreover, the impact on the perceived spectrum occupancy Ψ of particular parameters $\mathbf{p} = (p_1, p_2, \ldots, p_M)$ of the considered scenario and radio environment can easily be isolated, quantified and analyzed. Furthermore, it is possible to easily include the effects of potential propagation phenomena of real environments by means of the values of σ_{S_k}, which can readily be obtained experimentally with common measurement equipment, thus enabling more accurate and reliable estimations.

III. CONSIDERED SCENARIO AND PROPAGATION MODELS

The statistical prediction approach described in Section II is here applied to a realistic scenario. The considered scenario consists on a generic urban environment where buildings of height h_r(m) are deployed following a uniform layout with inter-building separation b(m) and street width w(m) as shown in Figure 2. The area under study comprises a grid of 5×5 buildings. A TV transmitter ($K = 1$ and $\alpha_k = 1$) with height h_b(m) and operating frequency $f = 800$ MHz is located d(km) apart (taking as a reference the geometrical center of the area under study). Within this scenario, CR nodes with antenna height $h_m = 2$ m may be located at the center of building rooftops (height is $h_r + h_m$), at the ground level between buildings (height is h_m), or inside buildings at any floor (height is $n \cdot h + h_m$, with n being the floor number and $h = 3$ m/floor). The considered locations represent various cases of practical interest and embrace a wide range of receiving conditions and levels of radio propagation blocking, ranging from direct line-of-sight at rooftops to severely blocked and faded signals at the ground level and inside buildings.

CR nodes intend to opportunistically access the spectrum band used by the primary transmitter, and to this end they sense the spectrum. The aim is to determine the spectrum occupancy that would be perceived by CR nodes within this scenario based on the approach presented in Section II.

The propagation losses L between the TV station and the different scenario's locations are estimated as follows. For CR nodes in building rooftops, the Okumura-Hata model [14, 15] is employed. This model is intended for receivers at the ground level or low heights. However, since it does not take into account the receiver's environment, it has been employed to estimate the received power at building rooftops. In order to reduce the estimation error, Hata's correction factor for open areas [15, eqs. 19-20] has been employed. For CR nodes at the ground level, the received power is computed based on the COST231 Walfisch-Ikegami model [16], which accounts for the receiver's surrounding environment to provide more accurate estimations. Both models were envisaged for cellular mobile communication systems but are valid for the considered operating frequency. In both cases, the expressions corresponding to large metropolitan areas are considered. For indoor CR nodes, losses are estimated based on the building penetration loss model for non-line-of-sight conditions described in [16]:

$$L(\mathrm{dB}) = L_{\mathrm{outside}}(\mathrm{dB}) + W_e + W_{ge} + \beta \cdot l - h \cdot G_h \quad (4)$$

where L_{outside} is the outside loss from the TV transmitter to the building's external wall at $h_m = 2$ m height above the ground (based on the COST231 Walfisch-Ikegami model), $W_e = 7$ dB is the loss in the externally illuminated wall at perpendicular penetration of $\phi = 90°$, $W_{ge} = 4$ dB is the additional loss in the external wall when $\phi = 0°$, $\beta = 0.6$ dB/m is the loss per distance between adjacent walls, l(m) is the perpendicular distance from the externally illuminated wall, $h = 3$ m/floor and $G_h = 1.6$ dB/m is the height gain.

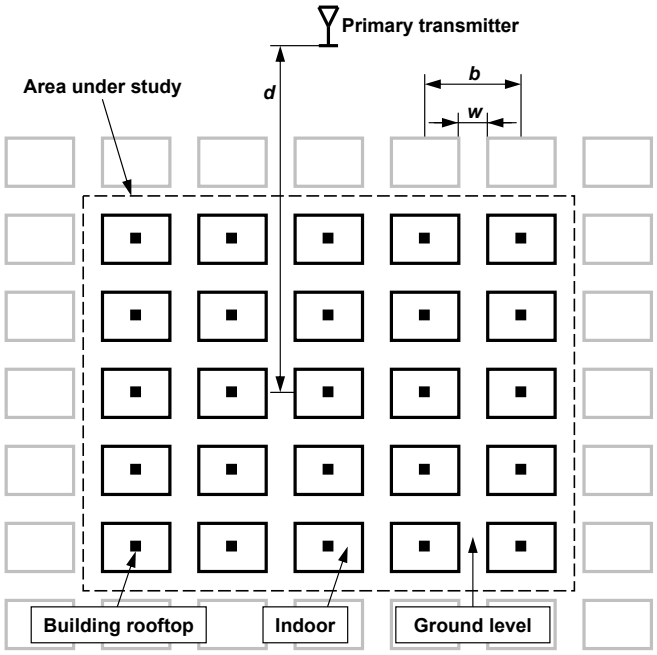

Fig. 2. Considered scenario.

IV. NUMERICAL RESULTS

This section analyzes how the proposed approach characterizes and describes the spectrum occupancy perceived by CR nodes of a DSA/CR network. Moreover, the users' perceived spectrum occupancy at different realistic locations as a function of the considered scenario and the surrounding radio propagation environment is also investigated.

Figure 3 shows the primary signal power P_S(dBm) received at various locations within the area under study, which has been computed based on the radio propagation models mentioned in Section III. As it can be appreciated, the highest

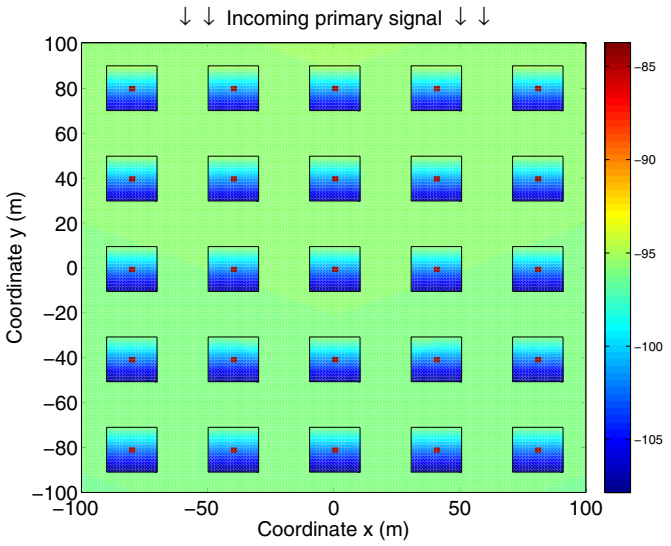

Fig. 3. Primary signal power $P_S(\mathrm{dBm})$ received at various locations within the area under study (P_T = 60 dBm, σ_S = 0.5252 dB, σ_N = 0.1679 dB, d = 4.8km, b = 40m, w = 20m, h_b = 50m, h_r = 40m, h_m = 2m, n = 3).

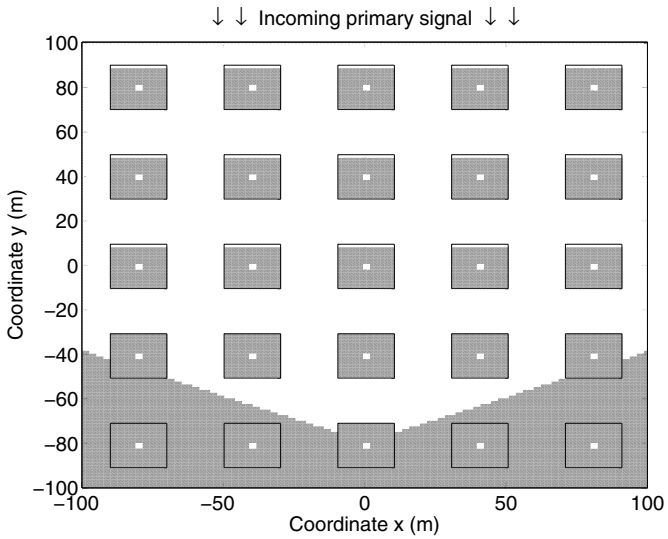

Fig. 4. Binary spectrum occupancy pattern perceived at various locations within the area under study (P_T = 60 dBm, σ_S = 0.5252 dB, σ_N = 0.1679 dB, P_{fa} = 0.01, NF = 8.6 dB, d = 4.8km, b = 40m, w = 20m, h_b = 50m, h_r = 40m, h_m = 2m, n = 3).

power level is observed at rooftops, as expected. It is interesting to note that the signal strength at that locations is slightly above the sensitivity of conventional TV receivers ($\approx -85\mathrm{dBm}$), meaning that the area under study (with the selected configuration parameters) can be considered to correspond to the border of the coverage area intended for the primary transmitter. As a result, primary users may be present within the area under study. The results of Figure 3 also indicate that the primary signal power received at the ground level and inside buildings suffers important attenuations with respect to rooftops, in the order of 10 and 20 dB respectively. This suggests that CR nodes within the same geographical area may experience quite dissimilar perceptions depending on their particular locations and propagation conditions.

To estimate the spectrum occupancy perceived within the considered scenario, and as a first approach, the power levels P_S(dBm) of Figure 3 are compared to a decision threshold in order to determine at which locations a CR node would decide that the spectrum is being used by the primary network. The decision threshold λ has been selected as [13]:

$$\lambda = P_N(\mathrm{dBm}) + Q^{-1}(P_{fa}) \cdot \sigma_N(\mathrm{dB}) \qquad (5)$$

in order to provide a probability of false alarm P_{fa} = 1%, which yields $\lambda \approx -96\mathrm{dBm}$ for the considered parameters' values. The results are shown in Figure 4, where the white and gray colors indicate that the primary signal is declared to be present or absent, respectively, at the corresponding location. At rooftops, where the highest power levels are observed, the primary signal is always detected according to this prediction approach. On the other hand, the signal appears to always be undetected in all indoor locations, where the lowest power levels are observed (excepting some buildings where the signal can be detected in indoor locations very near to the externally illuminated wall). At the ground level, the considered prediction approach indicates that the primary signal may be detected depending on the CR node's location. These results indicate that the considered simple approach is able to predict that, in the border of the primary coverage area (i.e., under low SNR conditions), there may be situations where primary users are present but secondary CR nodes may misdetect their transmissions, which would lead to potential situations of harmful interference. It is important to note, however, that the resulting characterization of the perceived spectrum occupancy is not only excessively simple but also unrealistic. In fact, Figure 4 shows, at the ground level, that this prediction approach indicates the existence of a hard limit such that the primary signal is always detected at locations slightly above, but never detected at locations slightly below.

In order to provide a more sophisticated and realistic characterization of the perceived spectrum occupancy, the statistical prediction approach of Section II is proposed. As shown in Figure 1, the P_S(dBm) values of Figure 3 are further processed in order to compute the probability that the sensed spectrum is observed as busy at various locations, based on the DC model of equation 1. This approach has been applied to the considered scenario with the same configuration parameters of Figure 4, resulting in the spectrum occupancy characterization shown in Figure 5. The same results are shown in Figure 6 in a three-dimensional view for ease of appreciation. Comparing Figure 4 with Figures 5 and 6, it can be observed that the two considered prediction approaches agree for locations at building rooftops and indoor environments, which can be considered as extreme cases in the sense that the highest and lowest primary signal powers are observed, respectively, at such locations. Thus, at rooftops (highest primary power), the simple approach predicts that the sensed spectrum is always observed as busy while the proposed approach indicates that this occurs with probability equal to one. At indoor locations (lowest primary power), the simple approach indicates that spectrum is always observed as idle, which is also corroborated by the proposed approach with a probability of observing the spectrum as busy approximately equal to zero. The differences between both approaches are observed in the spectrum occupancy perception predicted at the ground level. While the simple approach provides a simple binary characterization with a hard borderline, the proposed approach

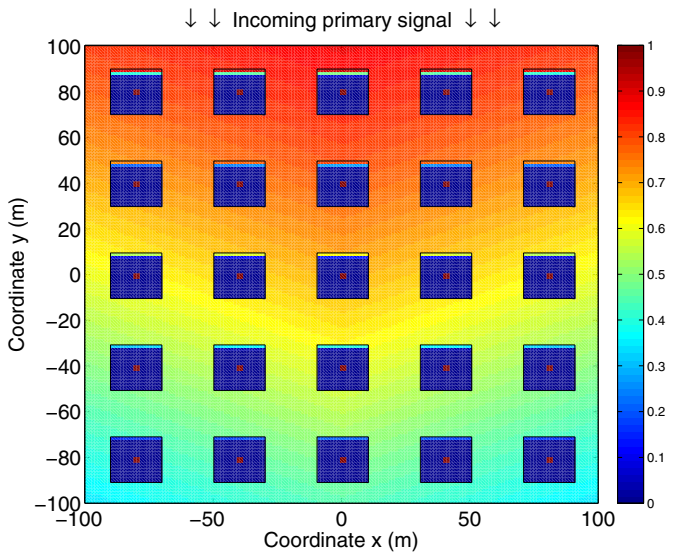

Fig. 5. Probabilistic spectrum occupancy pattern perceived at various locations within the area under study (P_T = 60 dBm, σ_S = 0.5252 dB, σ_N = 0.1679 dB, P_{fa} = 0.01, NF = 8.6 dB, d = 4.8km, b = 40m, w = 20m, h_b = 50m, h_r = 40m, h_m = 2m, n = 3).

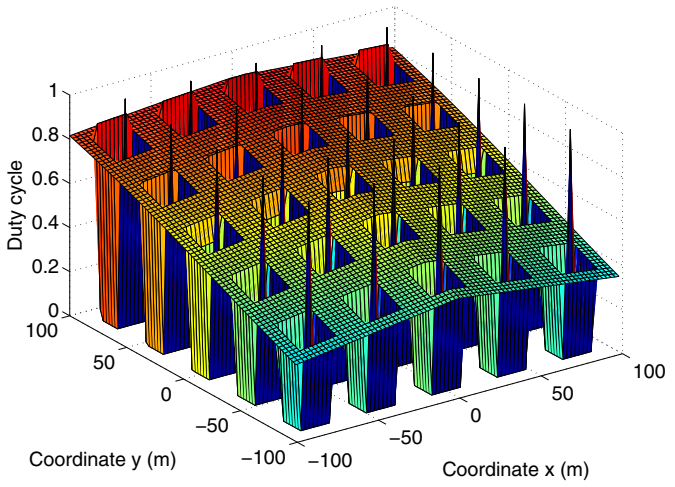

Fig. 6. Probabilistic spectrum occupancy pattern perceived at various locations within the area under study (P_T = 60 dBm, σ_S = 0.5252 dB, σ_N = 0.1679 dB, P_{fa} = 0.01, NF = 8.6 dB, d = 4.8km, b = 40m, w = 20m, h_b = 50m, h_r = 40m, h_m = 2m, n = 3).

provides a more sophisticated characterization by means of the probability that the spectrum is observed as busy, which increases progressively as the considered location approaches the primary transmitter (without observing any abrupt transitions). It is also interesting to note that, in some locations where the simple approach predicts the channel as always idle (busy), the proposed approach indicates that the probability of observing the channel as busy is low (high), but not equal to zero (one). This example shows how the proposed statistical prediction approach is able to provide a sophisticated and realistic characterization of the perceived spectrum occupancy as a function of the considered propagation scenario.

The proposed approach can also be used to study the impact of certain scenario and propagation parameters on the user's perception. Figures 7, 8 and 9 show some examples.

Figure 7 evaluates the impact of the transmitter and receiver antenna heights when the CR node is at the ground level. As expected, the detection performance improves as antenna heights increase, which results from the reduction of the radio propagation blocking caused by buildings. However, there are other interesting observations that can be inferred from the prediction provided by the proposed approach, and that would not have been possible with the simple approach considered as a reference. For example, Figure 7 indicates that the primary signal would not be detected for h_b < 42m, but it would always be detected for h_b > 46m, regardless of h_m. To guarantee that the primary signal is detected at the ground level with a probability of 0.9, the primary antenna height should be around 10m above the rooftop level (i.e., $h_b \approx h_r + 10m$) for the selected configuration parameters. For fixed h_b, the detection performance can be improved by increasing h_m. In this sense, it is interesting to note that Figure 7 indicates that the CR node's antenna height, h_m, should be increased about 1m for Medium-Small Cities (MSC) with respect to Large Cities (LC) in order to obtain the same detection performance. This can be explained by the fact that the COST231 Walfisch-Ikegami model employed to obtain Figure 7 includes an additional attenuation factor for the higher amount of vegetation usually present in MSCs.

Figure 8 shows the impact of building height and street width on the perceived spectrum occupancy for CR nodes at the ground level. Again, the detection performance improves as the radio propagation blocking becomes less significant, which in this case occurs for smaller buildings and wider streets. For example, for a fixed building height (e.g., h_r = 40m), the primary signal might be detected with probability close to one in wide streets (w = 25m) but it might be completely undetected in narrower streets (w = 15m). In general, the perceived spectral activity is higher in open areas than in narrow streets between buildings. It is worth noting that the trend shown in Figure 8 has also been observed empirically in the experimental study carried out in [8].

Finally, Figure 9 explores the spectrum occupancy perceived in indoor environments as a function of the distance from the externally illuminated wall l and floor number n. Compared to the user's perception at the ground level, the received primary signal strength in the indoor environment decreases faster with the distance. In fact, the signal would be detected close to the wall, but would be missed a few meters apart. The exact point where the signal begins to be undetected depends on the considered floor. As it can be observed, the perceived spectral activity is more significant in higher floors, which again can be related to a lower radio propagation blocking.

These few examples illustrate how the proposed approach can be employed not only to provide a statistical prediction of the spectral activity perceived by CR nodes, but also to quantify and analyze the impact of certain particular scenario and propagation parameters on the user's perception, which constitutes an important aspect in the design and dimensioning of DSA/CR systems in real deployments.

V. Conclusions

The behavior of a DSA/CR network, and consequently its impact on the primary network performance, strongly depends on the spectrum occupancy perceived by each CR node at its local environment. This work has proposed a novel and practical approach to predict the spectrum occupancy that

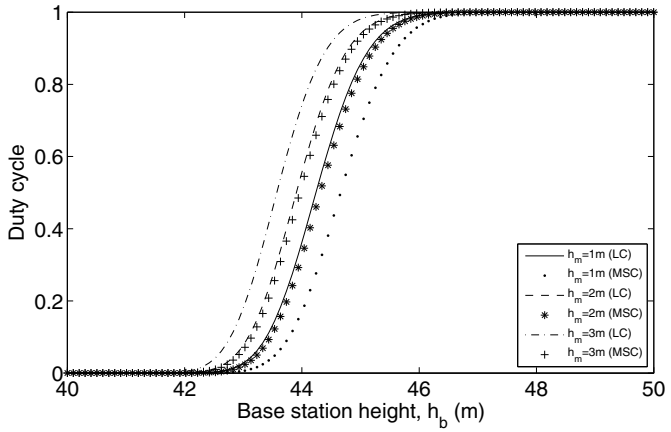

Fig. 7. Perceived spectrum occupancy at the ground level (P_T = 60 dBm, σ_S = 0.5252 dB, σ_N = 0.1679 dB, P_{fa} = 0.01, NF = 8.6 dB, d = 5km, b = 40m, w = 20m, h_r = 35m).

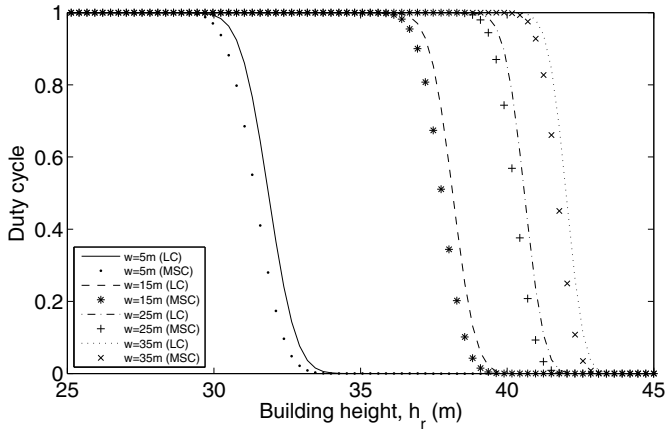

Fig. 8. Perceived spectrum occupancy at the ground level (P_T = 60 dBm, σ_S = 0.5252 dB, σ_N = 0.1679 dB, P_{fa} = 0.01, NF = 8.6 dB, d = 5km, b = 40m, h_b = 50m, h_m = 2m).

would be perceived by CR nodes in realistic scenarios. The user's perception is characterized in terms of the probability that the sensed spectrum is observed as busy, depending on the specific user's location, scenario and propagation environment. The impact on the perceived spectrum occupancy of particular factors and parameters can easily be isolated, quantified and analyzed with the proposed approach. The presented solution constitutes a valuable tool for the design, dimensioning and performance evaluation of DSA/CR networks.

ACKNOWLEDGEMENTS

This work was supported by the European Commission in the framework of the FP7 FARAMIR Project (Ref. ICT-248351) and the Spanish Research Council under research project ARCO (Ref. TEC2010-15198). The support from the Spanish Ministry of Science and Innovation (MICINN) under FPU grant AP2006-848 is hereby acknowledged.

REFERENCES

[1] M. A. McHenry *et al.*, "Spectrum occupancy measurements," Shared Spectrum Company, Tech. Rep., Jan 2004 - Aug 2005, available at: http://www.sharedspectrum.com.

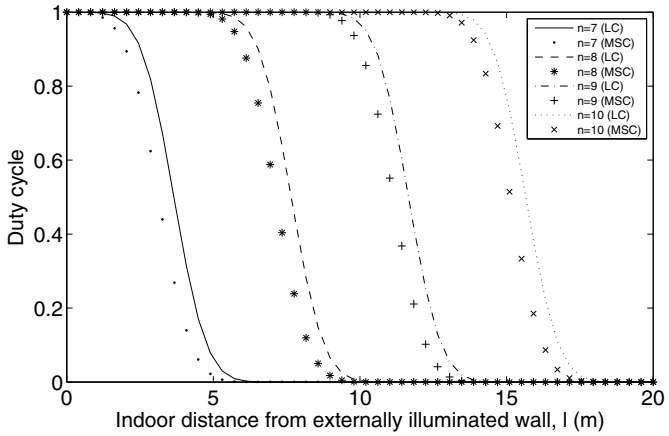

Fig. 9. Perceived spectrum occupancy at indoor locations (P_T = 60 dBm, σ_S = 0.5252 dB, σ_N = 0.1679 dB, P_{fa} = 0.01, NF = 8.6 dB, d = 5km, b = 40m, w = 20m, h_b = 50m, h_r = 40m, h_m = 2m).

[2] A. Petrin and P. G. Steffes, "Analysis and comparison of spectrum measurements performed in urban and rural areas to determine the total amount of spectrum usage," in *Proc. International Symposium on Advanced Radio Technologies (ISART 2005)*, Mar. 2005, pp. 9–12.

[3] R. I. C. Chiang, G. B. Rowe, and K. W. Sowerby, "A quantitative analysis of spectral occupancy measurements for cognitive radio," in *Proc. IEEE 65th Vehicular Technology Conference (VTC 2007 Spring)*, Apr. 2007, pp. 3016–3020.

[4] M. Wellens, J. Wu, and P. Mähönen, "Evaluation of spectrum occupancy in indoor and outdoor scenario in the context of cognitive radio," in *Proc. Second International Conference on Cognitive Radio Oriented Wireless Networks and Communications (CrowCom 2007)*, Aug. 2007, pp. 1–8.

[5] M. H. Islam *et al.*, "Spectrum survey in Singapore: Occupancy measurements and analyses," in *Proc. 3rd International Conference on Cognitive Radio Oriented Wireless Networks and Communications (CrownCom 2008)*, May 2008, pp. 1–7.

[6] M. López-Benítez, F. Casadevall, A. Umbert, J. Pérez-Romero, J. Palicot, C. Moy, and R. Hachemani, "Spectral occupation measurements and blind standard recognition sensor for cognitive radio networks," in *Proc. 4th International Conference on Cognitive Radio Oriented Wireless Networks and Communications (CrownCom 2009)*, Jun. 2009, pp. 1–9.

[7] I. F. Akyildiz, W.-Y. Lee, M. C. Vuran, and S. Mohanty, "NeXt generation/dynamic spectrum access/cognitive radio wireless networks: a survey," *Computer Networks*, vol. 50, no. 13, pp. 2127–2159, Sep. 2006.

[8] M. López-Benítez and F. Casadevall, "On the spectrum occupancy perception of cognitive radio terminals in realistic scenarios," in *Proc. 2nd IAPR International Workshop on Cognitive Information Processing (CIP 2010)*, Jun. 2010, pp. 1–6.

[9] H. Urkowitz, "Energy detection of unknown deterministic signals," *Proceedings of the IEEE*, vol. 55, no. 4, pp. 523–531, Apr. 1967.

[10] T. Yücek and H. Arslan, "A survey of spectrum sensing algorithms for cognitive radio applications," *IEEE Communications Surveys and Tutorials*, vol. 11, no. 1, pp. 116–130, 2009.

[11] D. D. Ariananda, M. K. Lakshmanan, and H. Nikookar, "A survey on spectrum sensing techniques for cognitive radio," in *Proc. of the Second International Workshop on Cognitive Radio and Advanced Spectrum Management (CogART 2009)*, May 2009, pp. 74–79.

[12] J. J. Lehtomaki, M. Juntti, H. Saarnisaari, and S. Koivu, "Threshold setting strategies for a quantized total power radiometer," *IEEE Signal Processing Letters*, vol. 12, no. 11, pp. 796–799, Nov. 2005.

[13] M. López-Benítez and F. Casadevall, "Spatial duty cycle model for cognitive radio," in *Proc. 21st Annual IEEE International Symposium on Personal, Indoor and Mobile Radio Communications (PIMRC 2010)*, Sep. 2010, pp. 1631–1636.

[14] Y. Okumura, E. Ohmori, T. Kawano, and K. Fukuda, "Field strength and its variability in VHF and UHF land-mobile radio service," *Review of the Electrical Communications Laboratory*, vol. 16, no. 9-10, pp. 825–873, Sep. 1968.

[15] M. Hata, "Empirical formula for propagation loss in land mobile radio services," *IEEE Transactions on Vehicular Technology*, vol. VT-29, no. 3, pp. 317–325, Aug. 1980.

[16] D. J. Cichon and T. Kürner, "Propagation prediction models (Digital mobile radio towards future generation systems, chapter 4)," COST231, Tech. Rep., Nov. 1998.